ORIGINAL ARTICLE
Urology

JKMS

https://doi.org/10.3346/jkms.2017.32.8.1327 • J Korean Med Sci 2017; 32: 1327-1336

# Identification of Downstream Genes of the mTOR Pathway that Predict Recurrence and Progression in Non-Muscle Invasive High-Grade Urothelial Carcinoma of the Bladder

**Subin Jin,[1]* In Ho Chang,[1]* Jin Wook Kim,[1] Young Mi Whang,[1] Ha Jeong Kim,[2] Soon Auck Hong,[3] and Tae-Jin Lee[4]**

[1]Department of Urology, Chung-Ang University College of Medicine, Seoul, Korea; [2]Department of Agricultural Biology, National Academy of Agricultural Science, Rural Development Administration, Jeonju, Korea; [3]Department of Pathology, Soonchunhyang University College of Medicine, Cheonan, Korea; [4]Department of Pathology, Chung-Ang University College of Medicine, Seoul, Korea

*Subin Jin and In Ho Chang contributed equally to this work.

Received: 18 March 2017
Accepted: 13 May 2017

Address for Correspondence:
Tae-Jin Lee, MD
Department of Pathology, Chung-Ang University College of Medicine, Chung-Ang University Hospital, 102 Heukseok-ro, Dongjak-gu, Seoul, 06973, Korea
E-mail: taejlee@cau.ac.kr

**Funding:** This research was supported by the Basic Science Research Program through the National Research Foundation of Korea (NRF) funded by the Ministry of Education, Science and Technology, Republic of Korea (2015R1A2A1A15054364), and also by the Chung-Ang University Research Scholarship Grants in 2016.

Microarray analysis was used to investigate the lack of identified mammalian target of rapamycin (mTOR) pathway downstream genes to overcome cross-talk at non-muscle invasive high-grade (HG)-urothelial carcinoma (UC) of the bladder, gene expression patterns, gene ontology, and gene clustering by triple (*p70S6K*, *S6K*, and *eIF4E*) small interfering RNAs (siRNAs) or rapamycin in 5637 and T24 cell lines. We selected mTOR pathway downstream genes that were suppressed by siRNAs more than 2-fold, or were up-regulated or down-regulated by rapamycin more than 2-fold. We validated mTOR downstream genes with immunohistochemistry using a tissue microarray (TMA) of 125 non-muscle invasive HG-UC patients and knockout study to evaluate the synergistic effect with rapamycin. The microarray analysis selected mTOR pathway downstream genes consisting of 4 rapamycin up-regulated genes (*FABP4*, *H19*, *ANXA10*, and *UPK3A*) and 4 rapamycin down-regulated genes (*FOXD3*, *ATP7A*, *plexin D1*, and *ADAMTS5*). In the TMA, FABP4, and ATP7A were more expressed at T1 and FOXD3 was at Ta. ANXA10 and ADAMTS5 were more expressed in tumors ≤ 3 cm in diameter. In a multivariate Cox regression model, ANXA10 was a significant predictor of recurrence and ATP7A was a significant predictor of progression in non-muscle invasive HG-UC of the bladder. In an *ATP7A* knock-out model, rapamycin treatment synergistically inhibited cell viability, wound healing, and invasion ability compared to rapamycin only. Activity of the *ANXA10* and *ATP7A* mTOR pathway downstream genes might predict recurrence and progression in non-muscle invasive HG-UC of the bladder. *ATP7A* knockout overcomes rapamycin cross-talk.

**Keywords:** Bladder Cancer; mTOR; Biomarker; Microarray; Recurrence; Progression

## INTRODUCTION

Mammalian target of rapamycin (mTOR) inhibitors are potently active against a wide variety of cancers. mTOR inhibitors could be useful in treatment of urothelial carcinoma (UC) of the bladder, since the inhibitors reduce cell viability in various cancer-derived cell lines and in a mouse model of UC of the bladder (1-3). We previously demonstrated that 2 mTOR downstream genes, *p70S6K* and *elF4E*, are involved in the regulation of cell proliferation to a similar extent, and inhibition of cells using a high dose of the mTOR inhibitor rapamycin effectively prevents in vitro and in vivo cellular growth in high-grade (HG)-UC of the bladder (4,5). We also reported that activation downstream of the mTOR pathway through phosphorylation by p70S6 kinase is related to high recurrence and progression in non-muscle invasive UC of the bladder (4-6). Despite such promising preclinical observations, clinical trials with mTOR inhibitors have proven disappointing (7,8). This might be due to cross-talk in the mTOR pathway leading to multiple sites of regulation and diverse genetic aberrations that activate the pathway.

Our aim was to identify downstream genes of the mTOR pathway that are transcriptionally altered due to mTOR pathway inhibition in UC cells using RNA interference (RNAi) and small molecule inhibitors. *p70S6K* and *elF4E* were knocked-down using 3 different small interfering RNAs (siRNAs) in 2 HG-UC cell lines (5637 and T24) that feature marked amplification and overexpression of downstream genes of the mTOR pathway, and since rapamycin targets the mTOR pathway. The downstream genes of the mTOR pathway identified in this study could be candidate targets for drug therapy that could overcome mTOR pathway cross-talk in non-muscle invasive HG-UC of the bladder.



pISSN 1011-8934
eISSN 1598-6357

## MATERIALS AND METHODS

### Cell cultures and reagents

Human HG-UC cell lines 5637 and T24 were purchased from the American Type Culture Collection (Manassas, VA, USA). Rapamycin was purchased from Sigma-Aldrich (St. Louis, MO, USA). Antibodies to p70 S6 kinase (gene name; *RPS6KB1*), phosphorylated-p70 S6 kinase (p-p70 S6 kinase, Ser371), eIF4E, phosphorylated-eIF4E (Ser209), and β-actin were purchased from Cell Signaling Technologies (Beverley, MA, USA). Antibody to ATP7A was purchased from Abcam (Cambridge, MA, USA). For generation of stable knockdown cell lines, plasmid *ATP7A* short-hairpin RNA (shRNA) constructs and a non-targeting shRNA control were purchased from Sigma-Aldrich. HG-UC 5637 cell line was transfected with either 5 μg of *ATP7A* shRNA plasmid DNA using Lipofectamine® 2000 (Invitrogen; Thermo Fisher Scientific Inc., Waltham, MA, USA) according to the manufacturer's instructions. Puromycin (0.1–1.0 μg/mL) was initiated 2 days after shRNA transfection.

### Cell viability analysis

Human HG-UC *ATP7A* knockdown 5637 cell lines were plated in 96-well plates in complete medium and treated with various concentrations of rapamycin. After 48 hours, cell viability was analyzed using the 3-(4,5-dimethylthiazol-2-yl)-2,5-diphenyltetrazolium bromide (MTT) assay according to the manufacturer's instructions (Sigma-Aldrich).

### Wound-healing migration assay

This assay was performed using the Cytoselect Wound Healing kit (Cell Biolabs, Inc., San Diego, CA, USA) according to the manufacturer's instructions. Cells of *ATP7A* knockdown and non-targeting shRNA control 5637 cell lines were plated in wells of a 6-well plate and incubated overnight to allow formation of a monolayer. The inserted wells were removed to create a wound field of 0.9 mm diameter. After washing, the cells were treated with 1 μM rapamycin and then incubated for 48 hours. The extent of wound closure was determined and photographed with a Zeiss 8 Axiovert 200M live cell microscope.

### Invasion assay

The cell invasion assay was performed with BioCoat™ Matrigel® Invasion Chambers 24-well plate (Corning Inc., Corning, NY, USA) according to the manufacturer's instructions. Briefly, the lower chambers contained 600 μL medium. *ATP7A* knockdown or non-targeting shRNA control 5637 cells were seeded in the upper chamber with 300 μL medium alone or medium containing 1 μM rapamycin. After 48 hours' incubation, non-invasive cells were removed from the upper chamber, and the adhered cells in the lower chamber were fixed in 4% paraformaldehyde for 20 minutes, stained with hematoxylin and enumerated using an upright microscope.

### Western blot analysis

Cells were washed with ice-cold phosphate-buffered saline and trypsinized prior to the addition of lysis buffer (iNtRON Biotechnology, Seoul, Korea). The lysates were stored at –20°C until analysis. The amount of protein was quantified by the Bradford assay (Bio-Rad, Hercules, CA, USA). Equal amounts of protein were loaded onto Readygels (4%–20% Tris-HCL; Bio-Rad), and electrophoresis was performed according to the manufacturer's instructions. Proteins were blotted onto polyvinylidene fluoride membranes (Invitrogen) and incubated for 1 hour at room temperature in 5% skim milk to blocking each membrane. Blots were incubated with primary antibody overnight at 4°C and with horseradish peroxidase-conjugated secondary antibody for 1 hour at room temperature. The membranes were developed using enhanced chemiluminescence.

### siRNA transfection

*p70S6K* siRNA (ID#: 6566, sense strand: 5′-GUGCCAAUCAGGUCUUUCU-3′, antisense strand: 5′-AGAAAGACCUGAUUGGCAC-3′) and eIF4E siRNA (ID#: 6311, sense strand: 5′-GGAUGGUAUUGAGCCUAUG-3′, antisense strand: 5′-CAUAGGCUCAAUACCAUCC-3′) were purchased from Cell Signaling Technologies. S6K siRNA (ID#: sc92312, sense strand 5′-CCUUCAACCACUAUCAGAAUU-3′, antisense strand: 5′-UUCUGAUAGUGGUUGAAGGUU-3′) were from Santa Cruz Biotechnology (Santa Cruz, CA, USA). Transient transfection of 5637 and T24 cells was performed using Lipofectamine® 2000 reagent (Invitrogen) according to the manufacturer's instructions.

### Microarray analysis

*Gene expression analysis using oligonucleotide microarrays*

For the control, and triple siRNA (*p70S6K, S6K,* and *eIF4E*), and rapamycin treated 5637 and T24 cells, the synthesis of target cRNA probes and hybridization were performed using Low RNA Input Linear Amplification kit (Agilent Technology, Palo Alto, CA, USA) according to the manufacturer's instructions. Amplified and labeled cRNA was purified on cRNA Cleanup Module (Agilent Technology) according to the manufacturer's protocol. The fragmented cRNA was resuspended in 2X hybridization buffer and directly pipetted onto assembled Agilent's Human Oligo Microarray (4 × 44K). The arrays were hybridized at 65°C for 17 hours using an oven (Agilent Technology). The hybridized microarrays were washed according to the manufacturer's washing protocol (Agilent Technology).

*Cutoffs*

The absolute cutoff value of fold-change had to be greater than 2.0 in at least 1 experiment, and the average intensity had to be greater than 300. These cutoffs reduced the number of genes

 https://doi.org/10.3346/jkms.2017.32.8.1327

from 8,976 to 234. Data were filtered to select genes that had both a proper fold change to remove the background of mostly unchanging genes and an average intensity distinguishable from the noise of microchip hybridization.

*Data acquisition and analysis*

The hybridized images were scanned using a DNA microarray scanner and quantified with Feature Extraction Software (Agilent Technology). All data normalization and the selection of genes with 2-fold change in expression were performed using GeneSpringGX 7.3 (Agilent Technology).

**Patient cohort and tissue microarray (TMA) construction**

We used 215 non-muscle-invasive UC bladder specimens collected at Chung-Ang University Hospital between 2005 and 2013 after obtaining Institutional Review Board approval. Paraffin blocks were available for 215 cases and TMAs were constructed using a manual array device (TMA set, Labro, Seoul, Korea) for 125 HG-UC samples. Two mm-thick tumor samples were collected in triplicate from each sample, and 4 μm-thick sections were consecutively incised from the recipient block and transferred to polylysine-coated glass slides. Because it was a retrospective study of anonymous patients, informed patient consent was waived. The study was carried out in agreement with the Declaration of Helsinki.

**Immunohistochemistry**

For the immunohistochemical procedures, 4 μm-thick sections were deparaffinized, rehydrated, and subjected to heat-induced antigen retrieval with a buffer solution using a streamer autoclave. Sections were then incubated with the appropriate primary antibody. After application of a secondary antibody, slides were developed using 3-3′-diaminobenzidine as a chromogen and counterstained with hematoxylin. TMA spots with artificial folds or those lacking target tissue representations were omitted from further analyses. The antibodies listed in Supplementary Table 1 were used. Tumor TMA spots stained with each marker were evaluated for extent (percent of positive cells) and intensity (0 to 3+ score). The standard H-score (scale 0–300) was calculated based on the product of percentage of stained cells (0–100) multiplied by staining intensity (1 = weak, 2 = moderate, and 3 = strong) (9). A final H-score was generated as the average of triplicate tissue samples. The H-scores of markers were used in the statistical analyses. In the Kaplan-Meier curve, a cutoff value of expression of each marker was used according to the median tumor H-score. In a Kaplan-Meier curve and Cox regression model, a cutoff value of the expression of each marker was used according to the median tumor H-score. Strong expression of a marker was defined as expression equal to or greater than the cutoff value, and weak expression as no expression or expression less than the cutoff value.

**Statistical analysis**

IBM SPSS ver. 21.0 (IBM Corp., Armonk, NY, USA) was used for all statistical analyses. The analysis of variance (ANOVA) test and Student's t-test were performed at $P < 0.05$ in order to identify genes that were differentially expressed across conditions. Hierarchical clustering was performed using similarity measurements based on Pearson correlations close to zero. Recurrence-free and progression-free survival (PFS) curves were estimated using the Kaplan-Meier method, and any differences in the survival curves were compared by log-rank tests. A Cox regression model was used to investigate predictive factors for the recurrence of HG-UC in a multivariate analysis.

## RESULTS

**Western blot of mTOR pathway expression after treatment with triple siRNAs or rapamycin in HG-UC cell lines**

We analyzed the expression of p70S6K and eIF4E proteins in 5637 and T24 UC cells. To study the downstream targets of the mTOR pathway, 5637 and T24 cell lines were treated with triple siRNAs (*p70S6K, S6K*, and *eIF4E*) or the mTOR inhibitor rapamycin (Fig. 1A). We evaluated protein expression after treatment with *p70S6K, S6K*, and *eIF4E* siRNAs in 5637 and T24 cells to confirm inhibition of *p70S6K* and *eIF4E* gene expression before performing complementary DNA (cDNA) microarray analysis. The triple siRNA treatment blocked the expression of *p70S6K* and *eIF4E* proteins in the 2 UC cell lines, and rapamycin inhibited the phosphorylation of p70S6K and eIF4E.

**Gene expression patterns after siRNA or rapamycin treatment**

In 5637 cells, 633 genes were down-regulated by triple siRNA treatment in comparison to the control. In T24 cells, 3,089 genes were down-regulated by triple siRNA treatment. We filtered reliable genes based on the objective criteria (Fig. 1B). The first filtering resulted in genes that were down-regulated by more than 2-fold compared to the control in response to triple siRNA treatment. The second filtering resulted in genes that were down-regulated or up-regulated by more than 2-fold in comparison to the control after rapamycin treatment. The third filtering excluded genes were upstream of the phosphoinositide 3-kinase (PI3K)/mTOR pathway. The fourth filtering removed genes with a low signaling spot (flags A, M). With the fifth filter, we selected genes related to the cell cycle.

Hierarchical cluster analysis was used to profile the gene expression patterns (Fig. 1C). In 5637 cells, 14 of the 42 genes included after the filtering process were rapamycin down-regulated genes and 28 genes were rapamycin up-regulated genes. In comparison, 27 of 43 genes in T24 cells were rapamycin down-regulated genes and 16 genes were rapamycin down-regulated genes. Two rapamycin down-regulated genes (*FABP4* and *H19*)

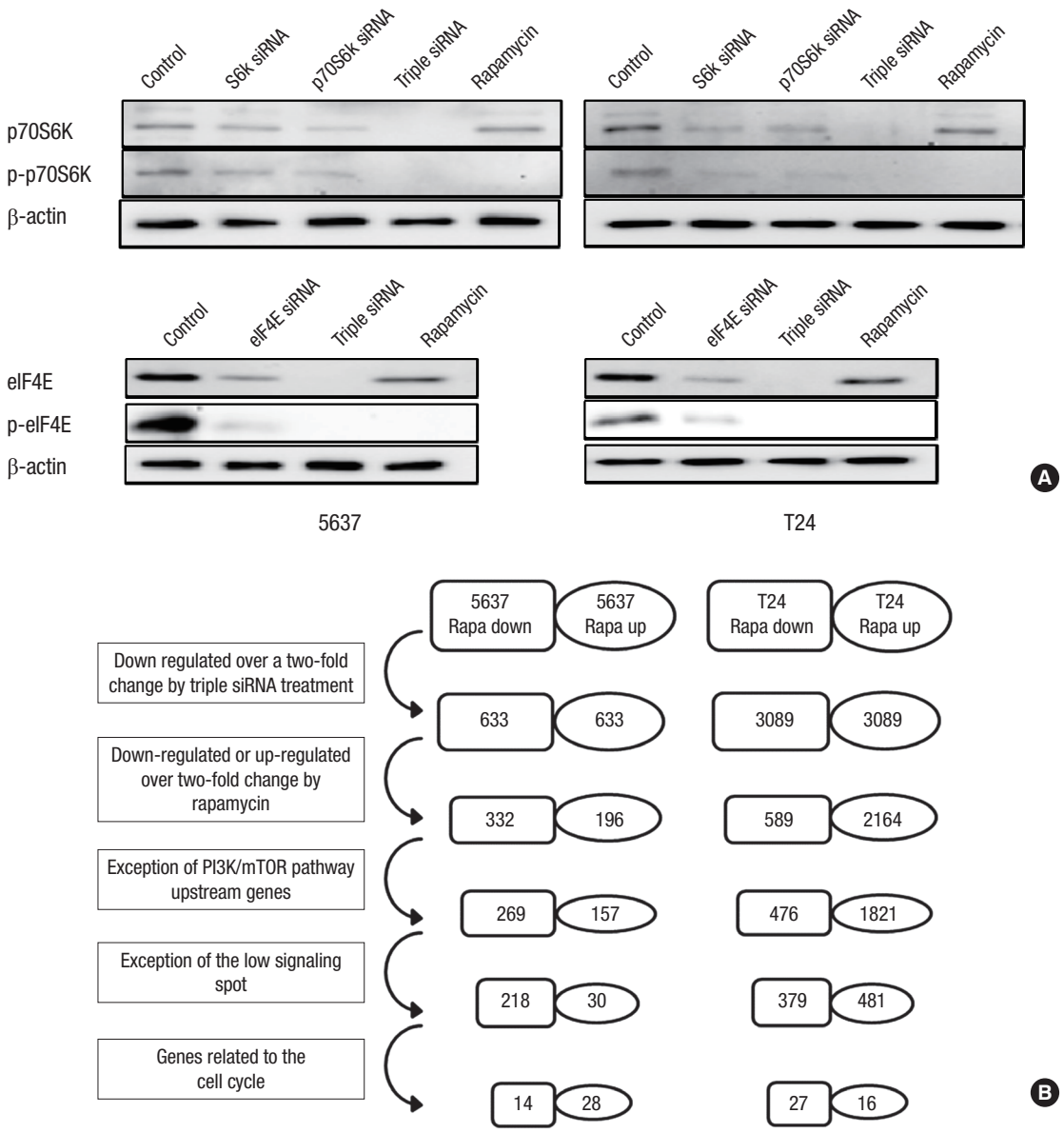


**Fig. 1.** Protein-level validation of p70S6K and eIF4E suppression after RPS6KB1 and eIF4E siRNA treatments, gene filtering, and gene expression profiling in HG-UC cell lines. (**A**) Reduced gene expression was observed in 5637 and T24 cells after transfection with siRNAs against p70S6K and eIF4E. Inhibited gene expression of both p70S6K and eIF4E was evident after treatment with triple siRNAs (p70S6K, S6K, and eIF4E). (**B**) Gene filtering process in 5637 and T24 cells.
siRNA = small interfering RNA, HG = high-grade, UC = urothelial carcinoma, PI3K = phosphoinositide 3-kinase, mTOR = mammalian target of rapamycin.

(Continued to the next page)

and 2 rapamycin up-regulated genes (*PLXND1* and *ADAMTS5*) were filtered from both the 5637 and T24 cell lines.

### Selection of mTOR pathway downstream genes according to gene expression pattern after siRNA or rapamycin treatment

Of 85 genes filtered from 5637 and T24 cells, we selected 4 that were simultaneously filtered from 5637 and T24 cells and 4 known to be associated with cancers based on a review of published studies (Table 1). *FABP4, H19, ANXA10*, and *UPK3A* were down-regulated by rapamycin and *FOXD3, ATP7A, PLXND1*, and *ADAMTS5* were rapamycin up-regulated genes. We investigated the gene ontology (GO) classes that were enriched in the gene expression profiles of RNAs and rapamycin-treated UC cell lines using the GO categorizer (Table 1) (10). In triple siRNA-treated UC cell lines, the representative enriched GO classes were functional categories involved in response organic substance (*FABP4*), immune response (*H19*), response calcium ion (*ANXA10*), potassium homeostasis (*UPK3A*), blood vessel morphogenesis (*PLXND1*), regulation of DNA binding (*FOXD3*), proteolysis (*ADAMTS5*), and blood vessel morphogenesis (*ATP7A*). Among these genes, *ANXA10, FOXD3*, and *ADAMTS5* were tumor sup-

 https://doi.org/10.3346/jkms.2017.32.8.1327

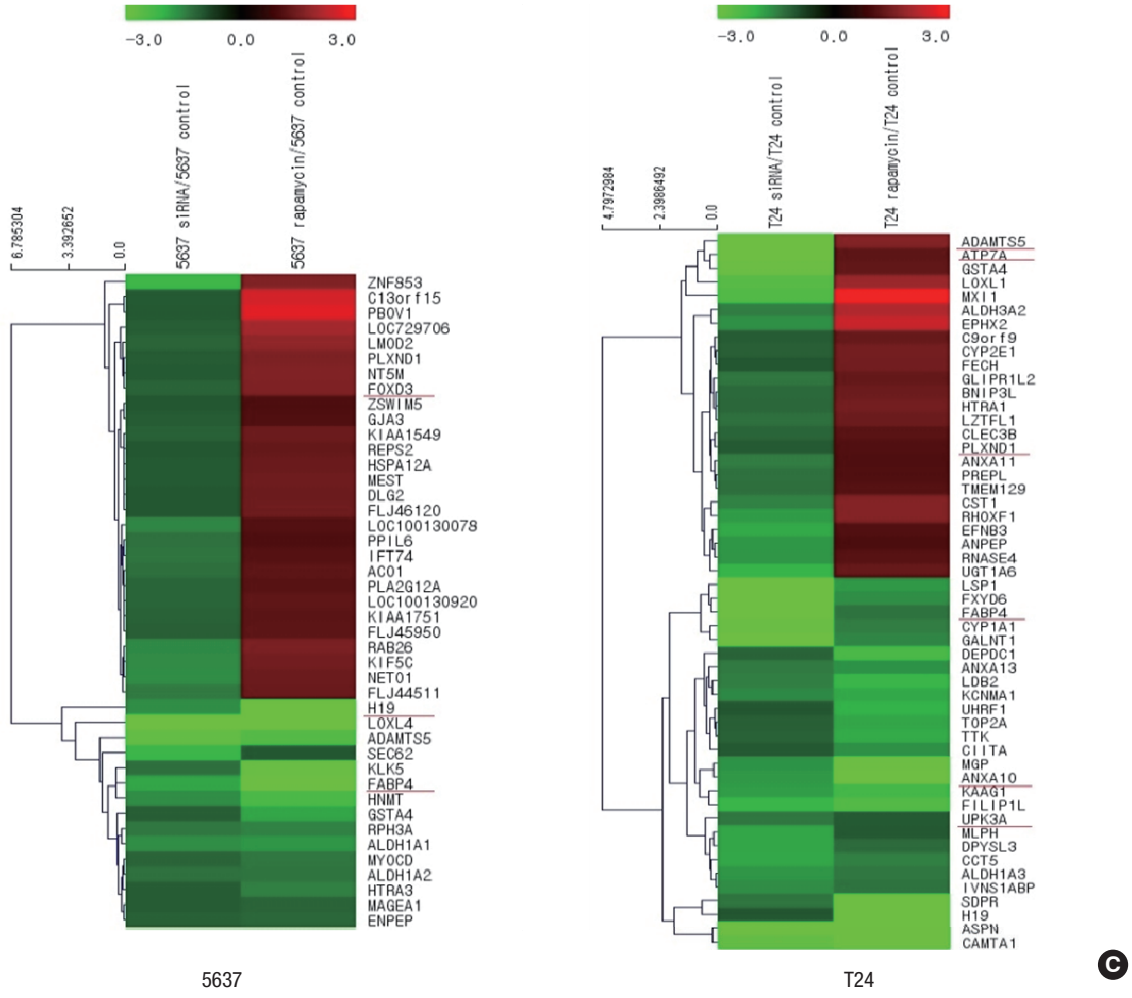


**Fig. 1.** (Continued) (**C**) Hierarchical clustering analysis of 5637 and T24 cells; red spots indicate up-regulation, green spots indicate down-regulation, black spots indicate an absence of modulation, and gray spots indicate the absence of values.

**Table 1.** Selection of mTOR pathway downstream genes according to the gene expression patterns after siRNAs or rapamycin treatment in HG-UC cell lines

| Gene name | Description | GO term | Expression by rapamycin |
|---|---|---|---|
| FABP4 | Fatty acid binding protein 4, adipocyte | Response to organic substance | D |
| H19 | H19, imprinted maternally expressed transcript (non-protein coding) | Immune response | D |
| ANXA10 | Annexin A10 | Response to calcium ion | D |
| UPK3A | Uroplakin 3A | Potassium ion homeostasis | D |
| PLXND1 | Plexin D1 | Blood vessel morphogenesis | U |
| FOXD3 | Forkhead box D3 | Regulation of DNA binding | U |
| ADAMTS5 | ADAM metallopeptidase with thrombospondin type 1 motif, 5 | Proteolysis | U |
| ATP7A | ATPase, $Cu^{++}$ transporting, alpha polypeptide | Blood vessel morphogenesis | U |

mTOR = mammalian target of rapamycin, siRNA = small interfering RNA, HG = high-grade, UC = urothelial carcinoma, GO = gene ontology, D = down-regulated expression, U = up-regulated expression.

pressor genes.

### Patient and tumor characteristics and expression of mTOR pathway downstream genes in relation to clinicopathological variables

FABP4, H19, ANXA10, UPK3A, FOXD3, ATP7A, PLXND1, and ADAMTS5 expression were detected by immunohistochemical staining in 115 (92.0%), 24 (19.2%), 119 (95.2%), 118 (94.4%), 119 (95.2%), 115 (92%), 102 (81.6%), and 99 (79.2%) of 125 non-muscle-invasive HG-UC samples, respectively (Fig. 2A). The median H-scores of FABP4, H19, ANXA10, UPK3A, FOXD3, ATP7A, PLXND1, and ADAMTS5 were 25.0, 0, 5.6, 13.3, 5.0, 30.0, 2.2, and 30.0, respectively.

The basic characteristics of the patients are shown in Supple-

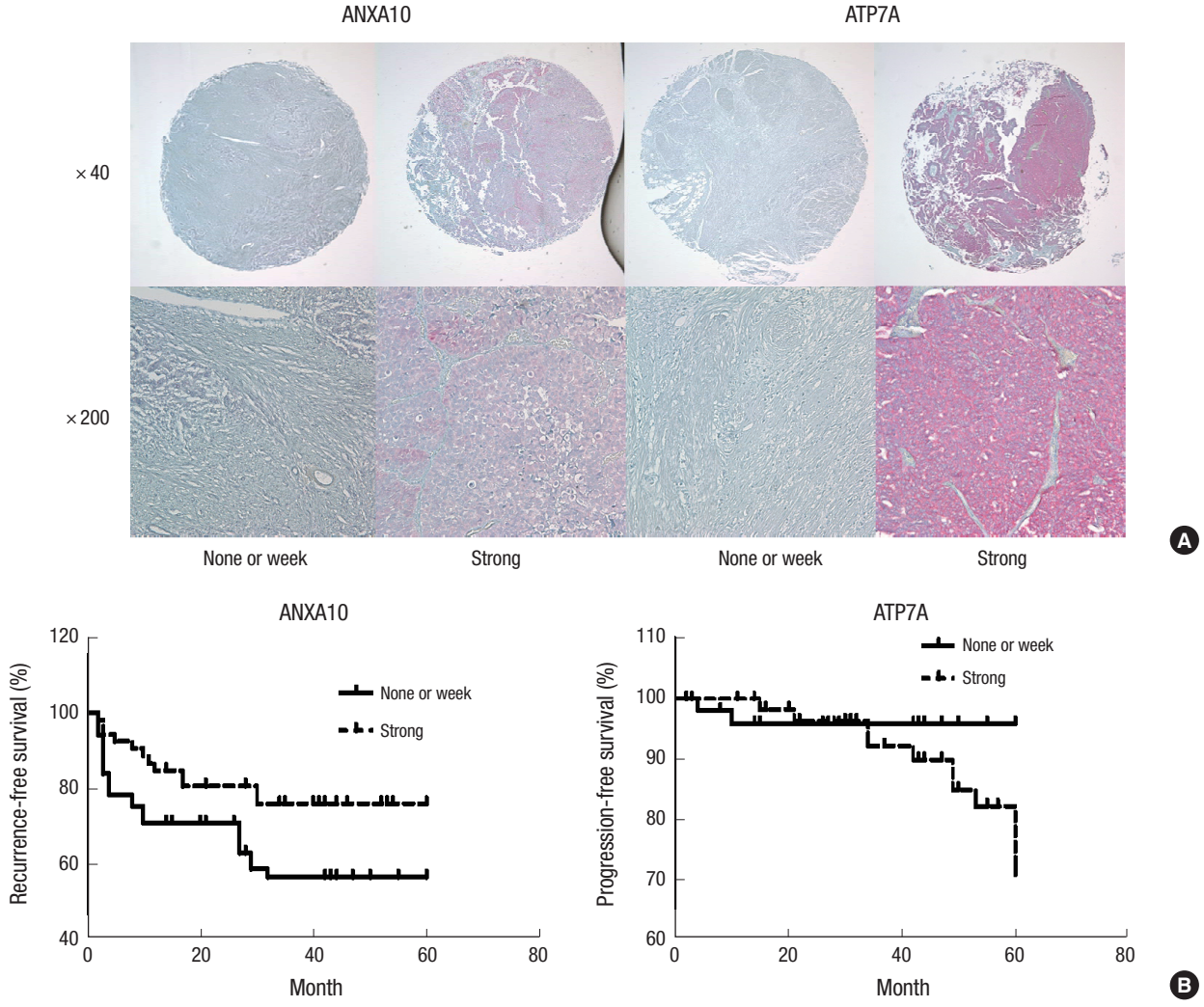


**Fig. 2.** Expression of downstream genes of the mTOR pathway in HG-UC of bladder tissues, and Kaplan-Meier curves based on staining results in HG-UC patients. (**A**) Immunohistochemical staining of ANXA10 and ATP7A in paraffin-embedded sections of HG-UC tissues (×40, ×200). (**B**) In RFS curves, HG-UC with no or weak ANXA10 immunohistochemical staining exhibited decreased RFS ($P$ = 0.037). In PFS curves, HG-UC with strong ATP7A immunohistochemical staining exhibited decreased PFS ($P$ = 0.004).
mTOR = mammalian target of rapamycin, HG = high-grade, UC=urothelial carcinoma, RFS = recurrence-free survival, PFS = progression-free survival.

mentary Table 2. The mean age was 66.7 years (range, 31–90) at the time of diagnosis of UC, and the median follow-up duration was 27 months (range, 2–60). Thirty-three patients (26.4%) had recurrence of UC within a mean follow-up of 36.5 months (range, 1–60). Thirteen patients (10.4%) developed a muscle-invasive disease within a mean period of 41.4 months (range, 3–60). Those aged 60–70 years comprised the largest number of patients (34.4%), and 88.8% of the patients were male. Primary tumors accounted for 28% of the prior recurrence rate. Single tumors were observed most frequently (60.8%) and a tumor size of ≤ 3 cm (59.2%) was observed more frequently than a tumor size > 3 cm. T1 cancer was present in 101 (80.8%) patients. A total of 57 patients (45.6%) received bacillus Calmette-Guérin (BCG) instillation as intravesical treatment.

Among the rapamycin down-regulated genes, FABP4 showed stronger expression in the T1 pathologic T stage than the Ta stage (H-score, 76.6 ± 25.5 vs. 49.4 ± 19.0; $P$ = 0.038), and ANXA10 showed weaker expression in tumors > 3 cm in size (H-score, 13.4 ± 6.7 vs. 39.6 ± 9.8; $P$ = 0.020) (Supplementary Table 2). Of the rapamycin up-regulated genes, ATP7A (H-score, 90.4 ± 30.7 vs. 59.0 ± 25.3; $P$ = 0.046) showed higher expression in T1 stage than Ta stage and FOXD (62.4 ± 22.2 vs. 86.8 ± 27.3; $P$ = 0.037) showed weaker expression; ADAMTS5 showed weaker expression in tumors larger than 3 cm (H-score, 12.0 ± 6.0 vs. 26.0 ± 13.0; $P$ = 0.014) (Supplementary Table 3).

In the Cox regression model, tumor multiplicity and none or weak *ANXA10* gene expression predicted shorter recurrence-free survival (RFS). And T1 stage, strong *FABP4*, and strong *ATP7A* gene expressions predicted shorter PFS in low-grade (LG)-UC in univariate analysis (Table 2). In multivariate analysis, tumor multiplicity (hazard ratio [HR], 2.173; $P$ = 0.017), and none or weak ANXA 10 (HR, 2.137; $P$ = 0.035) were independent fac-


https://doi.org/10.3346/jkms.2017.32.8.1327

**Table 2.** Cox proportional HR to identify predictive factors for recurrence and progression in HG-UC of the bladder

| Clinicopathologic factors | Cox proportional HR | | | | | | | |
|---|---|---|---|---|---|---|---|---|
| | Recurrence | | | | Progression | | | |
| | Univariate | | Multivariate | | Univariate | | Multivariate | |
| | RR (95% CI) | *P* value | RR (95% CI) | *P* value | RR (95% CI) | *P* value | RR (95% CI) | *P* value |
| Age (>70 yr) | 1.690 (0.893–3.200) | 0.107 | 1.625 (0.839–3.150) | 0.150 | 2.199 (0.751–6.438) | 0.150 | 2.392 (0.640–5.987) | 0.239 |
| Sex (male) | 0.714 (0.299–1.706) | 0.449 | 1.087 (0.427–2.768) | 0.861 | 1.473 (0.327–6.631) | 0.614 | 0.468 (0.083–2.629) | 0.388 |
| No. of tumors (multiple) | 2.152 (1.146–4.039) | 0.017 | 2.173 (1.151–4.100) | 0.017 | 0.392 (0.139–1.102) | 0.076 | 2.760 (0.939–8.109) | 0.065 |
| Tumor size (> 3 cm) | 1.083 (0.571–2.055) | 0.807 | 1.405 (0.724–2.726) | 0.315 | 1.180 (0.419–3.321) | 0.754 | 0.655 (0.206–2.082) | 0.473 |
| Tumor stage (T1) | 1.827 (0.898–3.750) | 0.101 | 1.805 (0.844–3.858) | 0.128 | 3.085 (1.050–9.065) | 0.040 | 1.985 (0.545–7.222) | 0.298 |
| FABP4 (> 25.0 H-score) | 1.380 (0.729–2.612) | 0.323 | - | - | 7.037 (1.587–31.210) | 0.010 | 3.072 (0.585–16.143) | 0.185 |
| H19 (> 0 H-score) | 0.625 (0.222–1.759) | 0.373 | - | - | 0.354 (0.047–2.696) | 0.316 | - | - |
| ANXA10 (≤ 5.6 H-score) | 2.069 (1.046–4.091) | 0.037 | 2.137 (1.055–4.328) | 0.035 | 1.309 (0.474–3.614) | 0.604 | - | - |
| UPK3A (> 13.3 H-score) | 0.852 (0.454–1.597) | 0.617 | - | - | 1.404 (0.499–3.948) | 0.948 | - | - |
| PLXND1 (> 5.0 H-score) | 0.973 (0.519–1.823) | 0.931 | - | - | 1.975 (0.675–5.782) | 0.214 | - | - |
| FOXD3 (> 30.0 H-score) | 1.514 (0.794–2.886) | 0.208 | - | - | 0.607 (0.208–1.788) | 0.363 | - | - |
| ADAMTS5 (> 2.2 H-score) | 0.658 (0.347–1.246) | 0.198 | - | - | 0.953 (0.346–2.631) | 0.927 | - | - |
| ATP7A (> 30.0 H-score) | 1.712 (0.897–3.267) | 0.103 | - | - | 8.830 (1.985–39.270) | 0.004 | 5.866 (1.106–31.102) | 0.038 |

HR = hazard ratio, HG = high-grade, UC = urothelial carcinoma, RR = relative risk, CI = confidence interval.

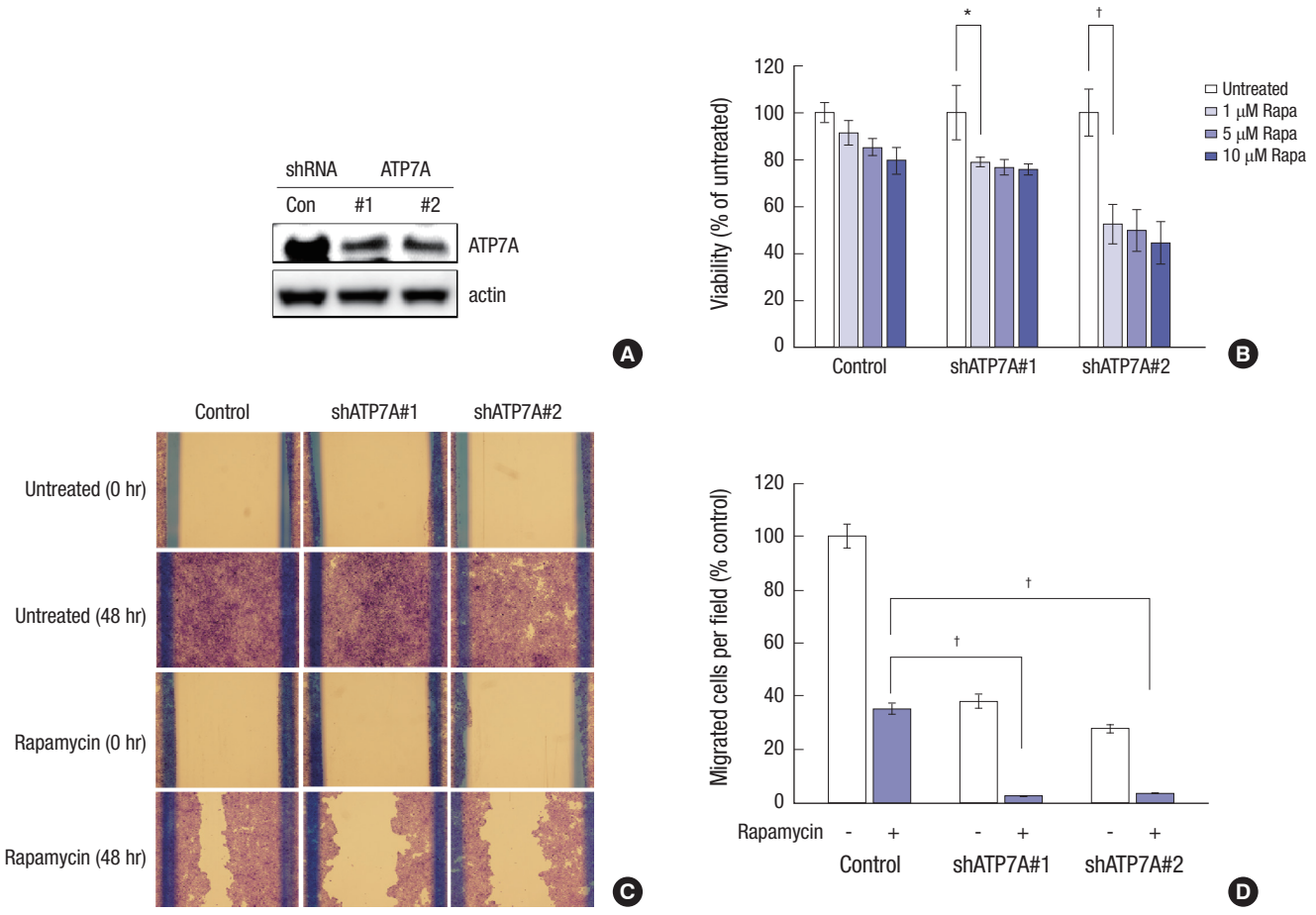


**Fig. 3.** Down-regulation of up-regulated ATP7A expression after siRNAs or rapamycin treatment in HG-UC 5637 cell line. (**A**) Western blots of whole-cell lysates from ATP7A stable knockdown and non-targeted shRNA control 5637 cell line after puromycin selection: control, pLKO.1 control vector; shATP7A#1 and shATP7A#2, ATP7A shRNA vectors. (**B**) Cell viability determined by MTT assay. Data are mean±SD (n = 6). (**C**) ATP7A stable knockdown 5637 cell lines exhibited reduced cell migration to rapamycin treatment. (**D**) ATP7A stable knockdown 5637 cell lines exhibited significantly reduced cell invasion compared to that of the control.
siRNA = small interfering RNA, HG = high-grade, UC = urothelial carcinoma, shRNA = short-hairpin RNA, MTT = 3-(4,5-dimethylthiazol-2-yl)-2,5-diphenyltetrazolium bromide, SD = standard deviation.
*$P < 0.050$, †$P < 0.010$.

tors predicting recurrence and strong *ATP7A* gene expression (HR, 5.866; $P = 0.038$) was an independent factor predicting progression (Table 2). In immunohistochemical staining, ANXA10 was expressed in the nucleus and cytoplasm of tumor cells and ATP7A was expressed in the cytoplasm of tumor cells, and non-muscle invasive HG-UC patients with none or week ANXA10 exhibited decreased RFS ($P = 0.037$), and strong ATP7A immunohistochemical staining exhibited decreased PFS ($P = 0.004$) in Kaplan-Meier's survival curve (Fig. 2A and B).

**Cell proliferation, wound healing, and invasion inhibition effect of rapamycin in ATP7A knockout 5637 cells**

The 5637 cells knocked-out for rapamycin up-regulated gene *ATP7A* were used to evaluate the synergistic effects of rapamycin and *ATP7A* inhibition. Two stable sh*ATP7A* RNA transfected 5637 cells (sh*ATP7A*#1 and sh*ATP7A*#2) were selected by Western blot analysis. Cell proliferation-inhibition effects of rapamycin were significantly increased in sh*ATP7A*#1 ($P < 0.023$) and sh*ATP7A*#2 ($P < 0.007$) compared with control in low concentration (1 μM) (Fig. 3A and B). The migration-inhibition effect of rapamycin was aggravated in *ATP7A* knockout 5737 cells compared to control (Fig. 3C). The invasion-inhibition effect of rapamycin was significantly exacerbated in *ATP7A* knockout 5637 cells compared to control at low rapamycin concentration (1 μM) ($P = 0.005$) (Fig. 3D).

## DISCUSSION

Since the mTOR pathway is associated with aggressive disease and poor prognosis of HG-UC, molecular profiling of genes suppressed downstream of the mTOR pathway might provide candidate molecular targets for new therapies. Gene expression patterns, GO, and gene clustering by triple siRNA (*p70S6K*, *S6K*, and *eIF4E*) or rapamycin treatment of 5637 and T24 cells were investigated using microarray analysis. We selected downstream genes of the mTOR pathway that were suppressed by over 2-fold and genes that were up- or down-regulated over 2-fold by rapamycin treatment. We then validated the expression of downstream genes of the mTOR pathway with immunohistochemistry using a TMA of 125 non-muscle invasive HG-UC patients to determine whether the genes predicted clinical aggressiveness and long-term outcome. Molecular profiling clustered UC of the bladder on the basis of histopathogenesis and biological criteria. The identified molecular targets were associated with histopathologic criteria and might become clinically useful biomarkers for the management of patients with UC of the bladder.

Our microarray data identified 2 rapamycin down-regulated genes (*FABP4* and *H19*) and 2 rapamycin up-regulated genes (*PLXND1* and *ADAMTS5*) that were altered due to mTOR pathway inhibition in UC cells using RNAi and small molecule inhibitors. These genes were functionally classified as encoding responses to organic substances (*FABP4*), immune response (*H19*), blood vessel morphogenesis (*PLXND1*), and proteolysis (*ADAMTS5*). This supports the hypothesis that the mTOR pathway is related to tumorigenesis because of its vital roles in cell growth, proliferation, and metabolism, indicating the successful implementation of the microarray. To our knowledge, this study is the first to show a molecular pattern associated with mTOR inhibition and specific to UC cell lines.

*ANXA10* and *ATP7A* were possible mTOR-related biomarkers for predicting tumor recurrence (*ANXA10*) and progression (*ATP7A*) of HG-UC in the multivariate Cox model. These results support several suggestions. The first is that these biomarkers might be capable of estimating the therapeutic efficacy of rapamycin. If the expression of *ATP7A* is high, the therapeutic efficacy of rapamycin to prevent recurrence or progression could be lower than usual. Rapamycin treatment may not be appropriate to prevent recurrence due the suppression of *ANXA10* in HG-UC patients with high *ANXA10* expression. Second, the biomarkers might be candidates for targeted therapy in HG-UC and could explain why rapamycin did not show high efficacy for HG-UC. In particular, the agonist for *ANXA10* and the inhibitor for *ATP7A* could be used as adjuvant treatment to rapamycin or new therapeutic agents for patients with rapamycin resistance.

*ANXs* are a family of calcium and phospholipid-binding proteins that share a similar structure characterized by the presence of 4 or 8 repeats of a 70-amino-acid motif and a highly variable N-terminal end (11). The *ANX* family is composed of 12 eukaryotic members that participate in diverse important biological and physiological processes including anti-coagulation, endocytosis, exocytosis, immune suppression, differentiation, and tissue growth (11-13). *ANXA10* was one of the markers included in the signature for predicting recurrence of non-muscle-invasive UC of the bladder, and low expression of *ANXA10* correlated with shorter RFS in patients with stage Ta and T1 tumors (14). Furthermore, patients with more advanced tumors and low *ANXA10* expression had an unfavorable prognosis (14).

The *ATP7A* gene product serves as a direct link between management of copper homeostasis and effective concentration of cisplatin in cells, and the *ATP7A* copper efflux ATPase pumps critically regulate cisplatin efflux (15,16). Thus, the uptake-efflux relative kinetics control intracellular accumulation of various drugs including cisplatin and, therefore, its cytotoxic action. *ATP7A* overexpression in cancer cells renders the cells resistant to drugs due to increased sequestration of the drug into the vesicular fraction, thus keeping the drug away from the target sites of its cytotoxic action (15,16). In our study, the higher expression of *ATP7A*, a rapamycin up-regulated gene, was related to predict higher progression in non-muscle invasive HG-UC of the bladder, and *ATP7A* knockout potentiated the

 https://doi.org/10.3346/jkms.2017.32.8.1327

cell proliferation, migration, and invasion inhibition effect of rapamycin. We suggest that up-regulated *ATP7A* inhibits uptake of mTOR inhibitor and the effect of drugs. *ATP7A* might be novel target to overcome the cross-talk of the mTOR pathway.

One of the limitations of this study was that tumor size and tumor stage were not related to progression and recurrence, although tumor multiplicity was related to recurrence in multivariate analysis. In the case of tumor size, the number of patients (n = 125) was smaller than other studies, and most patients with HG (84.2%) showed T1 stage, so we need more patients to validate the effects of tumor size and stage (17). And we need to discuss the effect of BCG because 45.6% of patients received BCG intravesical instillation to prevent recurrence and progression. We instilled intravesical BCG to patients with large size and high stage, and we hypothesis that the effect of BCG might interfere the effect of tumor size and stage (17).

Based on microarray and clinical characteristics, our results reveal that the *ANXA10* is an mTOR-related down-regulated biomarker and the low expression by mTOR inhibitor could predict recurrence in HG-UC of the bladder. So, we need to choose other treatment agents than mTOR inhibitor for bladder cancer when the expression of *ANXA10* is high. Also, *ATP7A* is a potential mTOR-related up-regulated biomarker and the high expression by mTOR inhibitor could predict progression in HG-UC of the bladder. Moreover, in our study, *ATP7A* knockout can potentiate the effect of mTOR inhibitor, which means that the resistance of mTOR inhibitor might be related with the rapamycin cross-talk and mTOR and *ATP7A* dual inhibitor might overcome rapamycin cross-talk. Since mTOR expression is associated with aggressive disease and poor prognosis of UC, molecular profiling of downstream genes of a suppressed mTOR pathway, which is associated with recurrence and progression of UC, might provide candidates for novel molecular target therapies. mTOR inhibitor could have clinical utility for preventing recurrence and progression in UC when rapamycin down-regulated genes are expressed in non-muscle-invasive UC of the bladder. The expression of rapamycin-up-regulated genes might predict recurrence and progression after rapamycin treatment, so new agents to inhibit these genes in combination with rapamycin treatment are needed. These genes might be useful target genes for novel targeted therapies and these studies might enable individualized therapies for non-muscle invasive UC of the bladder. Further in vitro and in vivo studies will evaluate the mechanisms and functions of these candidate genes and demonstrate clinical validation to advance individualized therapies.

## DISCLOSURE

The authors have no potential conflicts of interest to disclose.

## AUTHOR CONTRIBUTION

Conceptualization: Chang IH, Lee TJ. Data curation: Jin S, Kim HJ. Formal analysis: Kim JW. Investigation: Whang YM, Kim HJ. Supervision: Lee TJ. Writing - original draft: Jin S, Chang IH.

## ORCID

Subin Jin https://orcid.org/0000-0002-0779-8348
In Ho Chang https://orcid.org/0000-0003-0240-1310
Jin Wook Kim https://orcid.org/0000-0003-4157-9365
Young Mi Whang https://orcid.org/0000-0003-0437-204X
Ha Jeong Kim https://orcid.org/0000-0001-7353-575X
Soon Auck Hong https://orcid.org/0000-0002-7902-4608
Tae-Jin Lee https://orcid.org/0000-0002-0026-5936

## REFERENCES

1. Garcia JA, Danielpour D. Mammalian target of rapamycin inhibition as a therapeutic strategy in the management of urologic malignancies. *Mol Cancer Ther* 2008; 7: 1347-54.
2. Panwalkar A, Verstovsek S, Giles FJ. Mammalian target of rapamycin inhibition as therapy for hematologic malignancies. *Cancer* 2004; 100: 657-66.
3. Le Tourneau C, Faivre S, Serova M, Raymond E. mTORC1 inhibitors: is temsirolimus in renal cancer telling us how they really work? *Br J Cancer* 2008; 99: 1197-203.
4. Kwon JK, Kim SJ, Kim JH, Mee Lee KM, Chang IH. Dual inhibition by S6K1 and Elf4E is essential for controlling cellular growth and invasion in bladder cancer. *Urol Oncol* 2014; 32: 51.e27-35.
5. Chi BH, Kim SJ, Seo HK, Seo HH, Lee SJ, Kwon JK, Lee TJ, Chang IH. P70S6K and Elf4E dual inhibition is essential to control bladder tumor growth and progression in orthotopic mouse non-muscle invasive bladder tumor model. *J Korean Med Sci* 2015; 30: 308-16.
6. Kim SJ, Kim JH, Jung HS, Lee TJ, Lee KM, Chang IH. Phosphorylated p70S6K in noninvasive low-grade urothelial carcinoma of the bladder: correlation with tumor recurrence. *Asian J Androl* 2014; 16: 611-7.
7. Milowsky MI, Iyer G, Regazzi AM, Al-Ahmadie H, Gerst SR, Ostrovnaya I, Gellert LL, Kaplan R, Garcia-Grossman IR, Pendse D, et al. Phase II study of everolimus in metastatic urothelial cancer. *BJU Int* 2013; 112: 462-70.
8. Seront E, Rottey S, Sautois B, Kerger J, D'Hondt LA, Verschaeve V, Canon JL, Dopchie C, Vandenbulcke JM, Whenham N, et al. Phase II study of everolimus in patients with locally advanced or metastatic transitional cell carcinoma of the urothelial tract: clinical activity, molecular response, and biomarkers. *Ann Oncol* 2012; 23: 2663-70.
9. Detre S, Saclani Jotti G, Dowsett M. A "quickscore" method for immunohistochemical semiquantitation: validation for oestrogen receptor in breast carcinomas. *J Clin Pathol* 1995; 48: 876-8.
10. Heinonen H, Nieminen A, Saarela M, Kallioniemi A, Klefström J, Hautaniemi S, Monni O. Deciphering downstream gene targets of PI3K/mTOR/p70S6K pathway in breast cancer. *BMC Genomics* 2008; 9: 348.
11. Gerke V, Moss SE. Annexins: from structure to function. *Physiol Rev* 2002; 82: 331-71.

12. Hayes MJ, Moss SE. Annexins and disease. *Biochem Biophys Res Commun* 2004; 322: 1166-70.
13. Gerke V, Creutz CE, Moss SE. Annexins: linking $Ca^{2+}$ signalling to membrane dynamics. *Nat Rev Mol Cell Biol* 2005; 6: 449-61.
14. Munksgaard PP, Mansilla F, Brems Eskildsen AS, Fristrup N, Birkenkamp-Demtröder K, Ulhøi BP, Borre M, Agerbæk M, Hermann GG, Orntoft TF, et al. Low ANXA10 expression is associated with disease aggressiveness in bladder cancer. *Br J Cancer* 2011; 105: 1379-87.
15. Rabik CA, Dolan ME. Molecular mechanisms of resistance and toxicity associated with platinating agents. *Cancer Treat Rev* 2007; 33: 9-23.
16. Safaei R. Role of copper transporters in the uptake and efflux of platinum containing drugs. *Cancer Lett* 2006; 234: 34-9.
17. Choi SY, Ryu JH, Chang IH, Kim TH, Myung SC, Moon YT, Kim KD, Kim JW. Predicting recurrence and progression of non-muscle-invasive bladder cancer in Korean patients: a comparison of the EORTC and CUETO models. *Korean J Urol* 2014; 55: 643-9.


https://doi.org/10.3346/jkms.2017.32.8.1327